

# Structure of *Escherichia coli* glutamate decarboxylase (GAD $\alpha$ ) in complex with glutarate at 2.05 Å resolution

D. I. Dutyshev,<sup>a\*</sup> E. L. Darii,<sup>a</sup>  
N. P. Fomenkova,<sup>b</sup> I. V. Pechik,<sup>a</sup>  
K. M. Polyakov,<sup>a</sup> S. V. Nikonov,<sup>b</sup>  
N. S. Andreeva<sup>a</sup> and  
B. S. Sukhareva<sup>a</sup>

<sup>a</sup>V. A. Engelhardt Institute of Molecular Biology, RAS, 32 Vavilov Str., 119991 Moscow, Russia, and <sup>b</sup>Institute of Protein Research, RAS, 42290 Pushchino, Moscow Region, Russia

Correspondence e-mail:  
kostya@crystal.eimb.relarn.ru

Glutamate decarboxylase (GAD) is a pyridoxal enzyme that catalyzes the conversion of L-glutamate into  $\gamma$ -aminobutyric acid and carbon dioxide. The *Escherichia coli* enzyme exists as two isozymes, referred to as GAD $\alpha$  and GAD $\beta$ . Crystals of the complex of the recombinant isozyme GAD $\alpha$  with glutarate as a substrate analogue were grown in space group *R*3, with unit-cell parameters  $a = b = 117.1$ ,  $c = 196.4$  Å. The structure of the enzyme was solved by the molecular-replacement method and refined at 2.05 Å resolution to an *R* factor of 15.1% ( $R_{\text{free}} = 19.9\%$ ). The asymmetric unit contains a dimer consisting of two subunits of the enzyme related by a noncrystallographic twofold axis which is perpendicular to and intersects a crystallographic threefold axis. The dimers are related by a crystallographic threefold axis to form a hexamer. The active site of each subunit is formed by residues of the large domains of both subunits of the dimer. The coenzyme pyridoxal phosphate (PLP) forms an aldimine bond with Lys276. The glutarate molecule bound in the active site of the enzyme adopts two conformations with equal occupancies. One of the two carboxy groups of the glutarate occupies the same position in both conformations and forms hydrogen bonds with the N atom of the main chain of Phe63 and the side chain of Thr62 of one subunit and the side chains of Asp86 and Asn83 of the adjacent subunit of the dimer. Apparently, it is in this position that the distal carboxy group of the substrate would be bound by the enzyme, thus providing recognition of glutamic acid by the enzyme.

Received 16 September 2004

Accepted 3 December 2004

**PDB Reference:** GAD $\alpha$ -  
glutarate complex, 1key,  
r1xeyf.

## 1. Introduction

Pyridoxal phosphate (PLP) dependent amino-acid decarboxylases involved in the biosynthesis of biogenic amines play an important physiological role. Three-dimensional structures have been established for glycine decarboxylase (Faure *et al.*, 2000), DOPA decarboxylase (Malashkevich *et al.*, 1992, 1999), dialkylglycine decarboxylase (Toney *et al.*, 1993) and ornithine decarboxylases from various sources (Momany *et al.*, 1995; Grishin *et al.*, 1999; Kern *et al.*, 1999). Decarboxylases are classified into four groups based on comparative analysis of their amino-acid sequences (Sandmeier *et al.*, 1994). Glutamate decarboxylase (GAD; EC 4.1.1.15) belongs to the second group of these enzymes.

Glutamate decarboxylase is a pyridoxal enzyme that catalyzes the conversion of L-glutamate into  $\gamma$ -aminobutyric acid and carbon dioxide. This enzyme fulfils important physiological functions in humans and higher animals by balancing excitation and inhibition in the central nervous system and acting as an autoantigen in insulin-dependent diabetes. The *Escherichia coli* enzyme maintains pH under acidic conditions in the intestines. *E. coli* GAD exists as a hexamer with a

molecular weight of 316 kDa. The hexamer consists of six identical subunits (To, 1971), each subunit containing one PLP (Sukhareva & Braunstein, 1971). Two structural genes, *gadA* and *gadB*, were found in *E. coli* K-12. These genes encode two isozymes, GAD $\alpha$  and GAD $\beta$  (Smith *et al.*, 1992), which were expressed and purified (De Biase *et al.*, 1996; Shul'ga *et al.*, 1999). The natural enzyme has been crystallized previously (Markovic-Housley *et al.*, 1987; Sukhareva *et al.*, 1989) and preliminary X-ray diffraction analysis of the enzyme has been carried out. However, a more detailed study has not been performed. Investigations of recombinant GAD were more successful. After the preliminary study (Malashkevich *et al.*, 1998), the three-dimensional structure of the complex of the isozyme GAD $\beta$  with acetate was solved (Capitani *et al.*, 2003). In the present study, we established the three-dimensional structure of the GAD $\alpha$  complex with glutarate.

## 2. Materials and methods

Expression and purification of GAD $\alpha$  from the recombinant strain *E. coli* BL21(DE3)[pLys ED] were performed in principle as described by Shul'ga *et al.* (1999), but the final step involved dialysis against 0.1 M acetate buffer pH 4.6. The material was then passed through a short Sephadex G-25 fine column equilibrated with 0.1 M pyridine chloride buffer pH 4.6 containing 50 mM glutarate, 0.1 mM PLP, 1 mM dithiothreitol and 0.1 mM EDTA.

Crystallization was performed by the hanging-drop vapour-diffusion method (McPherson, 1982). The crystallization conditions were as follows: the drop consisted of 3  $\mu$ l of a

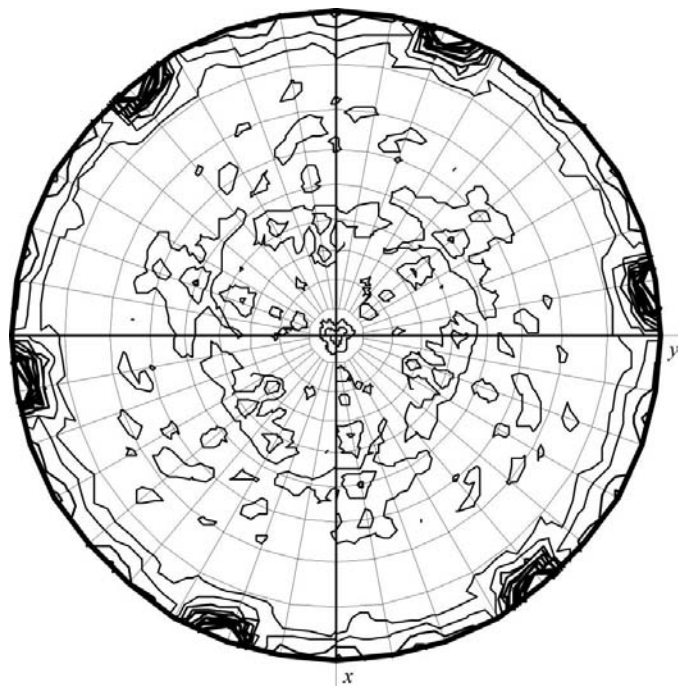


**Figure 1**  
Stereographic projection along the *z* axis of the self-rotation function for the twofold axis (peak heights corresponding to the noncrystallographic twofold axis are 76% of the height of the peak corresponding to the crystallographic threefold axis).

**Table 1**

Statistics of X-ray data collection and structure refinement.

The values for the last shell are given in parentheses.	
PDB code	1xye
Resolution range (Å)	29.00–2.05 (2.10–2.05)
$I/\sigma(I)$	9.97 (4.46)
Completeness (%)	95.6 (91.1)
$R_{\text{sym}}^{\dagger}$ (%)	9.1 (26.0)
Rf $^{\ddagger}$ (%)	15.1
$R_{\text{free}}^{\S}$ (%)	19.9
R.m.s. bond lengths (Å)	0.018
R.m.s. bond angles (°)	1.443
No. of atoms	7631
Protein	7168
PLP	30
Glutarate	30
Solvent and buffer	403
Average <i>B</i> factor (Å <sup>2</sup> )	
Protein main chain	21.85
Protein side chain	23.85
PLP	13.40
Glutarate	17.90
Solvent and buffer	26.67
Percentage of residues in Ramachandran plot regions $^{\P}$	
Most favoured	90.6
Additional allowed	9.2
Generously allowed	0.3

$^{\dagger} R_{\text{sym}} = \sum_h \sum_l |I_{h,l} - \langle I_h \rangle| / \sum_h \sum_l I_{h,l}$ , where  $\langle I_h \rangle$  is the average intensity of the symmetry-equivalent reflections; the summation was extended over all observations for all unique reflections.  $^{\ddagger} \text{Rf} = (\sum_h ||F_o| - |F_c||) / \sum_h |F_o|$ , where  $|F_o|$  and  $|F_c|$  are the observed and scaled calculated structure-factor amplitudes, respectively; the summation was extended over all unique reflections in the resolution range used.  $^{\S}$  For  $R_{\text{free}}$ , the summation was extended over a subset (5%) of reflections which were excluded in all stages of refinement.  $^{\P}$  Pro, Gly and terminal residues are omitted.

19.2 mg ml<sup>-1</sup> solution of GAD $\alpha$  in 0.1 M pyridine chloride buffer pH 4.6 containing 50 mM glutarate, 0.1 mM PLP, 1 mM dithiothreitol, 0.1 mM EDTA, 10% glycerol and 3  $\mu$ l of a reservoir solution composed of 7% PEG 3000 and 0.1 M NaCl in 0.1 M sodium acetate buffer pH 4.6; the temperature was 290 K. Both acetate and glutarate are inhibitors of glutamate decarboxylase from *E. coli*. However, their affinities for the enzyme are very different:  $k_i = 0.59$  mM for glutarate (Fonda, 1972a) and  $k_i = 20$  mM for acetate (Fonda, 1972b). Hence, the complex of GAD $\alpha$  with glutarate would be expected to be present in crystals obtained under these conditions. The crystals grew during 2–3 weeks as truncated trigonal pyramids with maximum dimensions of 0.2  $\times$  0.2  $\times$  0.5 mm. X-ray diffraction data were collected (at room temperature) using a MAR 345 imaging plate and a GX-6 rotating-anode generator (Eliot; Cu *K* $\alpha$  radiation,  $\lambda = 1.5418$  Å) at the Institute of Protein Research, RAS. The crystals belong to space group R3, with unit-cell parameters  $a = b = 117.1$ ,  $c = 196.4$  Å. X-ray diffraction data were collected to 2.05 Å resolution and processed using the *DENZO* and *SCALEPACK* programs (Otwinowski & Minor, 1997). The self-rotation function is shown in Fig. 1. The structure of the complex of GAD $\alpha$  with glutarate was solved by the molecular-replacement method using the *MOLREP* program (Vagin & Teplyakov, 1997). The monomer of the structure of GAD $\beta$  (PDB code 1pmm) was used as the starting model. Two rotation-function peaks were noticeably higher than all other peaks and the translation functions for both these peaks were solved. The asymmetric unit contains two monomers related by a noncrystallographic

twofold axis. The structure was refined using the *REFMAC* program (Murshudov *et al.*, 1997). Model building was carried out using the *TURBO-FRODO* program (Roussel & Cambillau, 1991). The statistics of X-ray data collection and structure refinement are summarized in Table 1.

### 3. Results and discussion

The primary structures of the two isozymes *GAD $\alpha$*  and *GAD $\beta$*  differ at the following five amino-acid residues: Gln3(Lys), Leu5(Gln), Leu6(Val), Phe9(Leu) and Ala22(Ser). In both subunits of the dimer of *GAD $\alpha$* , the side chain of Ala22 is well localized (the thermal parameters of the *C $\beta$*  atom in subunits *A* and *B* are 25.3 and 21.7 Å<sup>2</sup>, respectively). The side chain of Phe9 (the average thermal parameter for the atoms of this side chain is approximately 52.6 Å<sup>2</sup>) was only localized in subunit *B*. In the model of the structure, the coordinates of the amino-acid residues in the regions 1–3 and 452–466 and the side chains of residues 5 and 6 in both subunits of the dimer and also residue 4 and the side chain of residue 9 of the subunit *A* are lacking because the electron density corresponding to these residues is absent.

The secondary structure of the monomer of *GAD $\alpha$*  is shown in Fig. 2. The monomer consists of three domains referred to as the N-terminal (residues 1–57), large (residues 58–346) and small (residues 347–466) domains. The N-terminal domain is formed by two  $\alpha$ -helices labelled h1 (residues 6–14) and h2 (39–53). The large domain is composed of a central mixed-type seven-stranded  $\beta$ -sheet [residues 120–123 (b1), 156–159 (b2), 176–179 (b3), 202–207 (b4), 240–243 (b5) and 269–273 (b6) form parallel strands; residues 285–289 (b7) form an antiparallel strand] surrounded by eight  $\alpha$ -helices [residues 70–78 (h3), 91–107 (h4), 126–146 (h5), 165–172 (h6), 191–197 (h7), 220–234 (h8), 322–334 (h9) and 335–346 (h10)] and a  $\beta$ -hairpin [residues 301–312 (B1)]. The secondary structure of this domain is typical of fold type I PLP-dependent enzymes (Jansonius, 1998). The small domain contains three  $\alpha$ -helices [residues 347–357 (h11), 392–400 (h12) and 431–449 (h13)] and two  $\beta$ -hairpins [residues 363–382 (B2) and 408–424 (B3)]. In the crystal structure, a noncrystallographic twofold axis lies in the plane perpendicular to the crystallographic symmetry axis (at an angle of 10° to the *a* axis, Fig. 1) and intersects the crystallographic axis. Two crystallographically independent subunits related by the noncrystallographic symmetry axis form a dimer. The dimers are related by the crystallographic threefold axis to form a compact two-layer hexameric structure (Fig. 3). The large and small domains of one subunit belong to one layer, whereas the large and small domains of another subunit form another layer. The N-terminal domain of each subunit belongs to the same layer as the large and small domains of another subunit of the dimer.

The following contacts are made between the subunits in the dimer. Residues 27–32 of the N-terminal domain form contacts with  $\alpha$ -helix h4 of the large domain of the adjacent subunit. Residues 32–38 of the N-terminal domain are in contact with the N-terminus of  $\alpha$ -helix h10 and the C-terminus of  $\alpha$ -helix h9 of the large domain of the adjacent subunit.  $\alpha$ -Helix h2 and residues 54–57 of the N-terminal domain form contacts with  $\alpha$ -helices h3, h4 and h10 of the large domain of the adjacent subunit. Residues 65–70 and  $\alpha$ -helix h3 of the

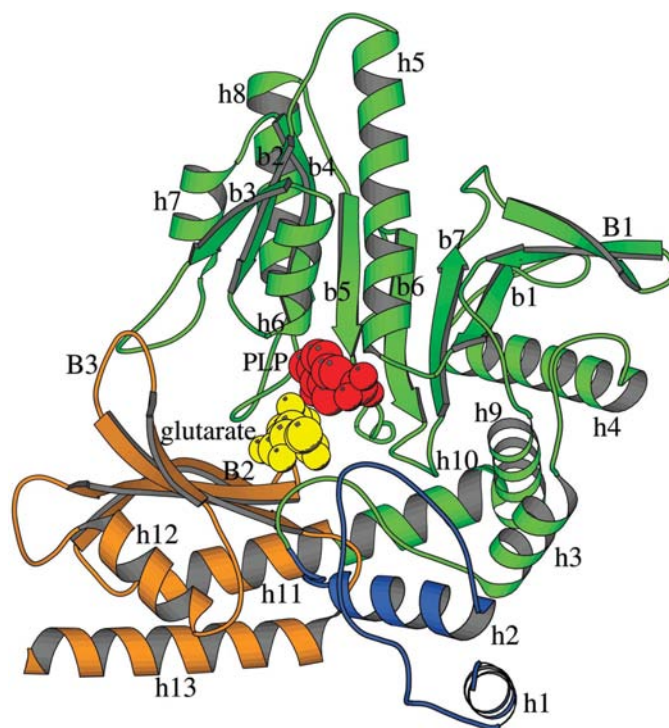


**Figure 2** Secondary structure of the monomer of *GAD $\alpha$* . The N-terminal, large and small domains are blue, green and orange, respectively. Glutarate and PLP are coloured yellow and red, respectively. The figure was prepared using the *MOLSCRIPT* program (Kraulis, 1991).

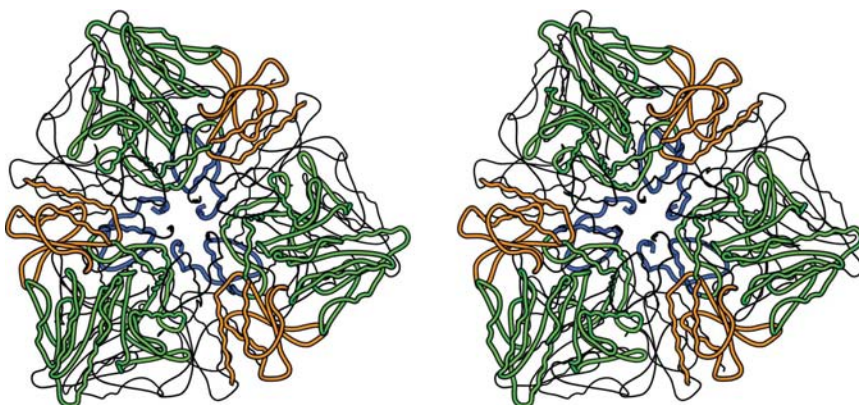


**Figure 3** Stereoview of the structure of the *GAD $\alpha$*  hexamer. The N-terminal, large and small domains are blue, green and brown, respectively. The *GAD $\alpha$*  monomers whose large and small domains belong to the lower layer of the hexamer are shown as thin lines. The orientation of the subunit in the lower layer of the *GAD $\alpha$*  hexamer presented in the upper part of the figure is identical to that presented in Fig. 2.



large domain are in contact with residues 65–70 and  $\alpha$ -helix h3 of the large domain of the adjacent subunit.  $\alpha$ -Helix h6 and residues 315–319 of the large domain form contacts with  $\alpha$ -helix h5 and residues 298–301 of the large domain of the adjacent subunit. The active site of each subunit is formed by residues of the large domain of this subunit and residues 83, 86 and 318 of the large domain of another subunit of the dimer. The r.m.s. deviation between the coordinates of the C $^{\alpha}$  atoms of the subunits of the dimer is 0.153 Å.

The hexamer is stabilized by contacts between subunits of the dimers related by the crystallographic threefold axis. The contacts formed by residues of the N-terminal domain make the major contribution to the formation of the hexamer. In addition to contacts between the subunits in the dimer, the following contacts are made between the amino-acid residues of the subunits in the hexamer.  $\alpha$ -Helix h1 and residues 15 and 16 of the N-terminal domain of each subunit form contacts with the analogous regions of the N-terminal domains of two other subunits belonging to the same layer of the hexamer. Residues 18–27 of the N-terminal domain of each subunit are in contact with residues 427–430 and the N-terminus of  $\alpha$ -helix h13 of the small domain of the subunit belonging to another layer of the hexamer.  $\alpha$ -Helix h2 and residues 54–57 of the N-terminal domain and residues 402–404 and  $\alpha$ -helix h13 of the small domain of each subunit form contacts with the analogous regions of the subunit belonging to another layer of

the hexamer.  $\alpha$ -Helix h12 of the small domain is in contact with  $\alpha$ -helix h12 of the small domain of the subunit belonging to another layer of the hexamer.

A comparison of the three-dimensional structures of GAD $\alpha$  and GAD $\beta$  (PDB code 1pmm) performed using the *LSQKAB* program (Kabsch, 1976), demonstrated that these isozymes are structurally very similar (r.m.s. deviations between the corresponding C $^{\alpha}$  atoms are about 0.4 Å). The distances between the superimposed C $^{\alpha}$  atoms of residues 4–12 (monomers *A*, *C* and *E* of GAD $\beta$ ), 114, 148, 149, 306, 307, 385 and 386 of two isozymes are as large as 1 Å. However, the thermal parameters of the atoms of these residues are also high and these atoms are located on the surface of the hexamers. The differences for amino-acid residues 4–12 of monomers *A*, *C* and *E* of GAD $\beta$  (which belong to the same layer) are attributable to the presence of contacts with the adjacent hexamers, whereas these amino-acid residues in the other layer of the hexamer in the structure of GAD $\beta$  and in the structure of GAD $\alpha$  are not involved in contacts with other hexamers. The regions containing residues 148 and 149 form van der Waals contacts with various regions of other hexamers (with amino-acid residues 178, 179 and 196 in the structure of GAD $\alpha$  and with residue 146 in GAD $\beta$ ). The distance between the C $^{\alpha}$  atoms of residue 54 are larger than 2 Å because the conformation of this residue was changed during the course of structure refinement.

The positions of PLP and glutarate in the active site of GAD $\alpha$  were revealed (Figs. 4 and 5*a*). The  $\epsilon$ -amino-acid group of Lys276 forms an aldimine bond with the aldehyde group of PLP. The phosphate group of PLP is involved in the following hydrogen bonds: the OP1 atom forms hydrogen bonds with Ser126 N, Ser127 OG and His275 NE2, the OP2 atom forms hydrogen bonds with the N and OG atoms of Ser318\* of the adjacent subunit of the dimer and the OP3 atom forms hydrogen bonds with Ser126 N and Ser127 N. Asp243 OD2 is involved in a hydrogen bond with the N1 atom of PLP. There is also a hydrophobic interaction between the side chain of Gln163 and the pyridine ring of PLP.

The main distinguishing feature of the complex of GAD $\alpha$  with glutarate is that the glutarate in each subunit adopts two different conformations (I and II) with occupancies of 0.5 (Figs. 4, 5*a* and 5*b*). The positions of one of the carboxyl groups of the glutarate are virtually identical in both conformations. This group forms hydrogen bonds with Phe63 N and Thr62 OG1 of one subunit and with Asn83\* ND2 and Asp86\* OD2 of the adjacent subunit of the dimer. This position of the carboxyl group of glutarate is identical to the position of the carboxyl group of the acetate molecule in the structure of GAD $\beta$  (PDB code 1pmm). In conformation I, the second carboxyl group of the glutarate is oriented toward the side chains of Lys276 and Gln163. One of the O atoms of this carboxyl group forms a hydrogen bond with Lys276 NZ and another O atom is at a distance of 3.5 Å from Gln163 NE2. Presumably, these atoms could form a hydrogen bond upon a slight conformational change. In conformation II, the second carboxyl group of the glutarate is oriented toward the side chain of Arg422 and forms hydrogen bonds with Arg422 NH2

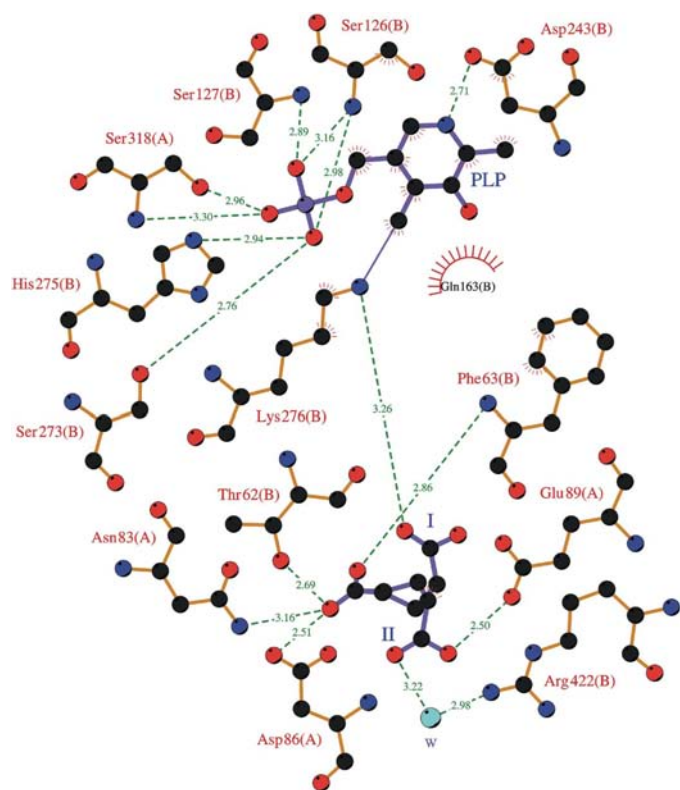


**Figure 4**

Scheme of the active site in GAD $\alpha$ . The C, O and N atoms are black, red and blue, respectively. The glutarate and PLP molecules are coloured violet. Hydrogen bonds are indicated by green dashed lines. The figure was generated using the *LIGPLOT* program (Wallace *et al.*, 1995).

through the water molecule and with Glu89\* OE2 of the adjacent subunit of the dimer.

We believe that the former carboxyl group of glutarate, which occupies virtually equivalent positions in two conformations, corresponds to the position of productive binding of the distal carboxyl group of the substrate (glutamic acid). In

this position, the carboxyl group of glutarate is more strongly bound to the enzyme compared with the carboxyl groups in two other positions and hence this mode of binding of the carboxyl group is essential for recognition of the substrate by the enzyme. Besides, if the  $\alpha$ -carboxyl group of glutamic acid were bound in this position, the distance between the C4 atom of PLP and the C $^{\alpha}$  atom of glutamic acid would be 5.5 Å and decarboxylation would be accompanied by substantial conformational changes in the active site of GAD $\alpha$ .

The positions of the carboxyl group of glutarate in the vicinity of Gln163 (conformation I) and in the vicinity of Arg422 (conformation II) cannot serve as a good model for productive binding of the  $\alpha$ -carboxyl group of glutamic acid by the enzyme. Binding of the  $\alpha$ -carboxyl group of glutamic acid in the vicinity of the second carboxyl group of glutarate is nonproductive because the latter is remote from PLP and Lys276 (conformation II). In the case of binding of the  $\alpha$ -carboxyl group of glutamic acid in the vicinity of Gln163 (conformation I), the conformation of glutamic acid is also nonproductive because the N atom of glutamic acid and PLP are located on opposite sides of the substrate. The position of the  $\alpha$ -carboxyl group of glutamic acid favourable for its productive binding in the active site of the enzyme is determined primarily by a covalent bond between the N atom of glutamic acid and the C4 atom of PLP.

This work was supported by Russian Foundation for Fundamental Research grant No. 02-04-49106 and the President's Program of Support of the Leading Scientific Schools (HIII-1781.2003.04).

References

Capitani, G., De Biase, D., Aurisi, K., Gut, H., Bossa, F. & Grütter, M. G. (2003). *EMBO J.* **22**, 4027–4037.  
 De Biase, D., Tramonti, A., John, R. A. & Bossa, F. (1996). *Protein Expr. Purif.* **8**, 430–438.  
 Faure, M., Bourguignon, J., Neuburger, M., Macherel, D., Sieker, L., Ober, R., Kahn, R., Cohen-Addad, C. & Douce, R. (2000). *Eur. J. Biochem.* **267**, 2890–2898.  
 Fonda, M. (1972a). *Biochemistry*, **11**, 1304–1309.  
 Fonda, M. (1972b). *Arch. Biochem. Biophys.* **153**, 763–768.  
 Grishin, N. V., Osterman, A. L., Brooks, H. B., Phillips, M. A. & Goldsmith, E. J. (1999). *Biochemistry*, **38**, 15174–15184.  
 Jansonius, J. N. (1998). *Curr. Opin. Struct. Biol.* **8**, 759–769.  
 Kabsch, W. (1976). *Acta Cryst.* **A32**, 922–923.

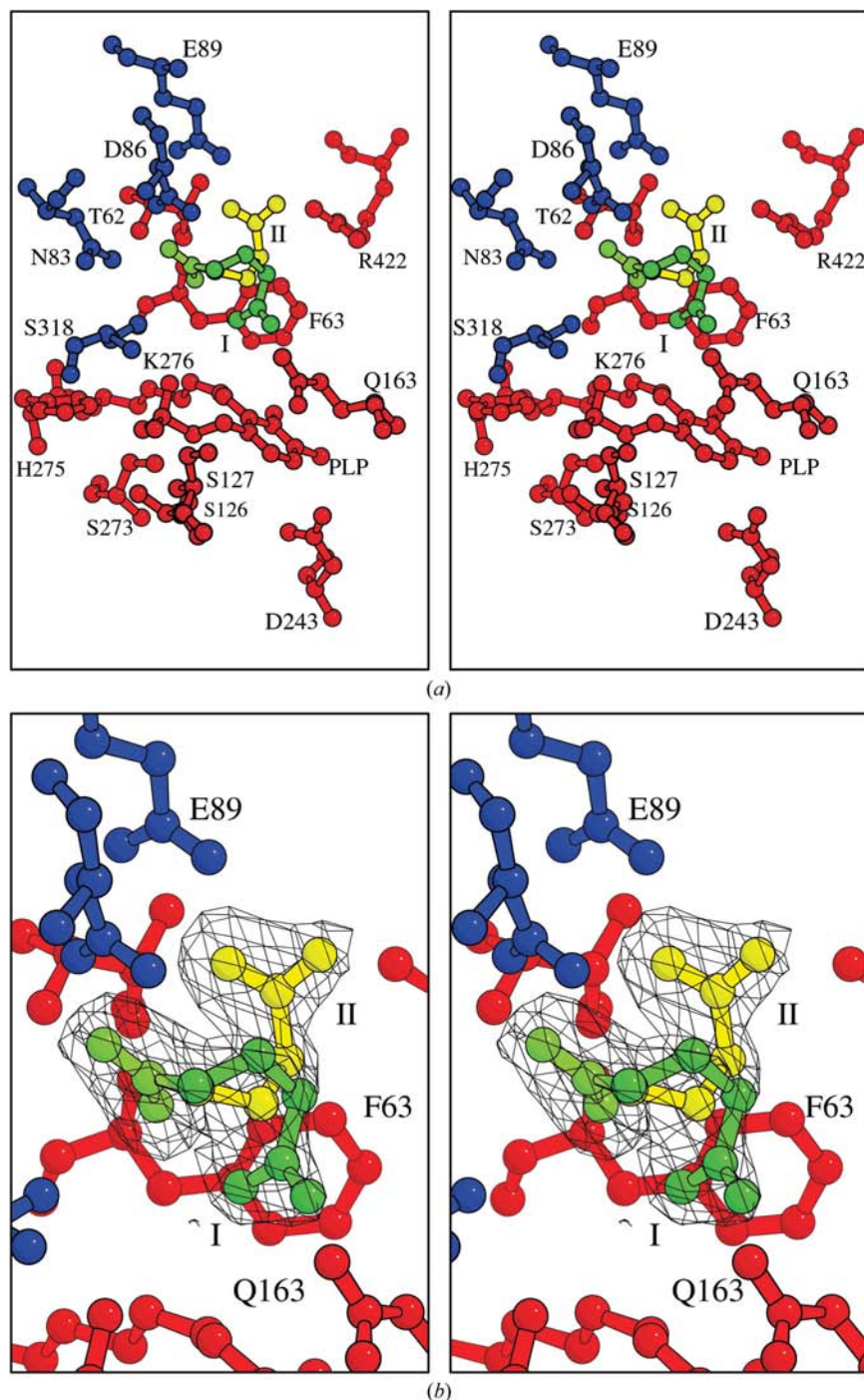


**Figure 5**  
 Stereoview of the active site of GAD $\alpha$ . (a) The atomic model of the active site. Glutarate is coloured green (conformation I) and yellow (conformation II), while the amino-acid residues belonging to the adjacent subunit of the dimer are in blue. (b) The electron density of the glutarate molecule ( $F_o - F_c$  map at the  $3\sigma$  level calculated without the contribution of the glutarate molecule). The omit electron density of the glutarate was calculated after 20 cycles of refinement for the final model without the glutarate atoms.

- Kern, A. D., Oliveira, M. A., Coffino, P. & Hackert, M. L. (1999). *Structure*, **7**, 567–581.
- Kraulis, P. J. (1991). *J. Appl. Cryst.* **24**, 946–950.
- McPherson, A. (1982). *Preparation and Analysis of Protein Crystals*. New York: John Wiley.
- Malashkevich, V. N., Burkhard, P., Dominici, P., Moore, P. S., Borri Voltattorni, C. & Jansonius, J. N. (1999). *Acta Cryst.* **D55**, 568–570.
- Malashkevich, V. N., De Biase, D., Markovic-Housley, Z., Schlunegger, M. P., Bossa, F. & Jansonius, J. N. (1998). *Acta Cryst.* **D54**, 1020–1022.
- Malashkevich, V. N., Filipponi, P., Sauder, U., Dominici, P., Jansonius, J. N. & Borri Voltattorni, C. (1992). *J. Mol. Biol.* **224**, 1167–1170.
- Markovic-Housley, Z., Kania, M., Vincent, M. G., Jansonius, J. N. & John, R. A. (1987). *Biochemistry of Vitamin B<sub>6</sub>*, edited by T. Korpela & P. Christen, pp. 187–190. Basel: Burkhäuser Verlag.
- Momany, C., Ernst, S., Ghosh, R., Chang, N.-L. & Hackert, M. L. (1995). *J. Mol. Biol.* **252**, 643–655.
- Murshudov, G. N., Vagin, A. A. & Dodson, E. J. (1997). *Acta Cryst.* **D53**, 240–255.
- Otwinowski, Z. & Minor, W. (1997). *Methods Enzymol.* **276**, 307–326.
- Roussel, A. & Cambillau, C. (1991). *Silicon Graphics Geometry Partners Directory*, p. 81. Mountain View, CA, USA: Silicon Graphics.
- Sandmeier, E., Hale, T. I. & Christen, P. (1994). *Eur. J. Biochem.* **221**, 997–1002.
- Shul'ga, A. A., Kurbanov, F. T., Khristoforov, R. R., Darii, E. L. & Sukhareva, B. S. (1999). *Mol. Biol. (Moscow)*, **33**, 560–566.
- Smith, D. K., Kassam, T., Singh, B. & Elliot, J. F. (1992). *J. Bacteriol.* **174**, 5820–5826.
- Sukhareva, B. S. & Braunstein, A. E. (1971). *Mol. Biol. (Moscow)*, **5**, 302–317.
- Sukhareva, B. S., Darii, E. L., Goryunov, A. I., Tyul'kova, N. A. & Malikova, L. G. (1989). *Biokhimiya (Moscow)*, **54**, 740–744.
- To, C. M. (1971). *J. Mol. Biol.* **59**, 215–217.
- Toney, M. D., Hohenester, E., Cowan, S. W. & Jansonius, J. N. (1993). *Science*, **261**, 756–759.
- Vagin, A. & Teplyakov, A. (1997). *J. Appl. Cryst.* **30**, 1022–1025.
- Wallace, A. C., Laskowski, R. A. & Thornton, J. M. (1995). *Protein Eng.* **8**, 127–134.